

<sup>2</sup>Sammons, G. D., "Study of the Thermal Behaviour of Solid-Propellants by Differential Scanning Calorimetry," *Analytical Chemistry*, Plenum Press, New York, 1968, pp. 305-311.

<sup>3</sup>Kishore, K., Pai Verneker, V. R., and Nair, M. N. R., "Condensed-Phase Reactions in Solid Propellant Combustion," *AIAA Journal*, Vol. 13, Sept. 1975, pp. 1,240-1,242.

<sup>4</sup>Pai Verneker, V. R., Kishore, K. and Nair, M. N. R., "Importance of Condensed-Phase Reactions in Solid-Propellant Combustion," Paper No. 75-1202, AIAA/SAE 11th Propulsion Conference, Anaheim, Calif., Sept. 29-Oct. 1, 1975.

<sup>5</sup>Pai Verneker, V. R., Kishore, K. and Mohan, V. K., "Correlation between Combustion and Decomposition of Solid-Propellants," *AIAA Journal*, Vol. 13, Oct. 1975, pp. 1415-1416.

<sup>6</sup>Rastogi, R. P., Kishore, K., and Singh, G., "Combustion of Polystyrene and Styrene-Oxygen Copolymer/ $\text{NH}_4\text{ClO}_4$  Propellants," *AIAA Journal*, Vol. 12, Jan. 1974, pp. 9-10.

<sup>7</sup>Kishore, K., Pai Verneker, V. R., and Mohan, V. K., "Differential Scanning Calorimetric Studies on the Thermal Decomposition of Ammonium Perchlorate," *Thermochimica Acta*, Vol. 13, 1975, pp. 277-292.

<sup>8</sup>Kishore, K., Pai Verneker, V. R. and Nair, M. N. R., "Thermal Degradation of Polystyrene," *Journal of Applied Polymer Science*, (In press).

<sup>9</sup>Jacobs, P. W. M. and Kuveisky, A. R. T., "Kinetics of Thermal Decomposition of Podium Azide," *Journal of the Chemical Society*, 1964, pp. 4718-4723.

## Compressible Laminar Boundary Layers with Large Acceleration and Cooling

Lloyd H. Back\* and Robert F. Cuffel†  
Jet Propulsion Lab., California Institute of Technology, Pasadena, Calif.

### Nomenclature

$a_{T_0}$	= sound speed at reservoir condition
$c_D$	= mass flow coefficient
$c_f$	= friction coefficient, $(c_f/2) = (\tau_w/\rho_e u_e^2)$
$D$	= diameter
$f'$	= dimensionless velocity, $u/u_e$
$f''_w$	= gradient at surface in transformed coordinates
$F$	= correlation function, Eq. (3)
$g_w$	= surface to total gas enthalpy, $H_w/H_{T_0}$
$G$	= dimensionless total enthalpy difference, Ref. 5
$H$	= static enthalpy
$H_T$	= total enthalpy, $H + u^2/2$
$M$	= Mach number
$r_w$	= body or channel radius
$r_{th}$	= throat radius
$r_c$	= throat radius of curvature
$Re_{\bar{\theta}}$	= momentum thickness Reynolds number, $\rho_e u_e \bar{\theta}/\mu_e$
$Re_{D_{th}}$	= throat Reynolds number, $(\rho_e u_e D/\mu_e)_{th}$
$T$	= temperature
$u$	= velocity component parallel to surface
$x$	= distance along surface
$y$	= distance normal to wall
$z$	= axial distance
$\beta$	= acceleration parameter in transformed coordinates, Ref. 5

Received June 30, 1975; revision received December 14, 1975. This work presents the results of one phase of research carried out in the Propulsion and Materials Research Section of the Jet Propulsion Laboratory, California Institute of Technology, under Contract NAS7-100, sponsored by the National Aeronautics and Space Administration.

Index categories: Boundary Layers and Convective Heat Transfer; Nozzle and Channel Flow.

\*Member Technical Staff, Associate Fellow AIAA.

†Member Technical Staff, Member AIAA.

$\beta\theta_t^2$

= acceleration parameter, Eq. (3)

$\gamma$

= specific heat ratio

$\delta^*$

= boundary-layer thickness,  $[1 - (\rho u/\rho_e u_e)]$

$\delta^*$

= displacement thickness,

$$r_w^j \delta^* = \delta^* (r_w - \delta^* \cos \sigma/2)^j$$

$$= \int_0^\infty [(1 - (\rho u/\rho_e u_e))] (r_w - y \cos \sigma)^j dy$$

$\delta_t^*$

= transformed displacement thickness, Eq. (5)

$\eta$

= dimensionless transformed coordinate normal to surface

$\bar{\theta}$

= momentum thickness,

$$r_w^j \bar{\theta} = \theta (r_w - \theta \cos \sigma/2)^j$$

$$= \int_0^\infty (\rho u/\rho_e u_e) (1 - u/u_e) (r_w - y \cos \sigma)^j dy$$

$\theta_t$

= transformed momentum thickness, Eq. (5)

$\mu$

= viscosity

$\nu$

= kinematic viscosity

$\rho$

= density

$\sigma$

= angle between wall and axis

$\tau_w$

= surface shear stress

### Subscripts

$e$

= condition at freestream edge of boundary layer

$o$

= reservoir condition

$T$

= stagnation condition

$th$

= throat condition

$w$

= surface condition

### Introduction

THIS Note is concerned with extending an approximate prediction method involving the integral form of the momentum equation<sup>1</sup> to deduce the flow quantities of interest when compressibility effects become important and heat transfer may occur. The approximate method is applicable to a two-dimensional, laminar boundary layer on an im-

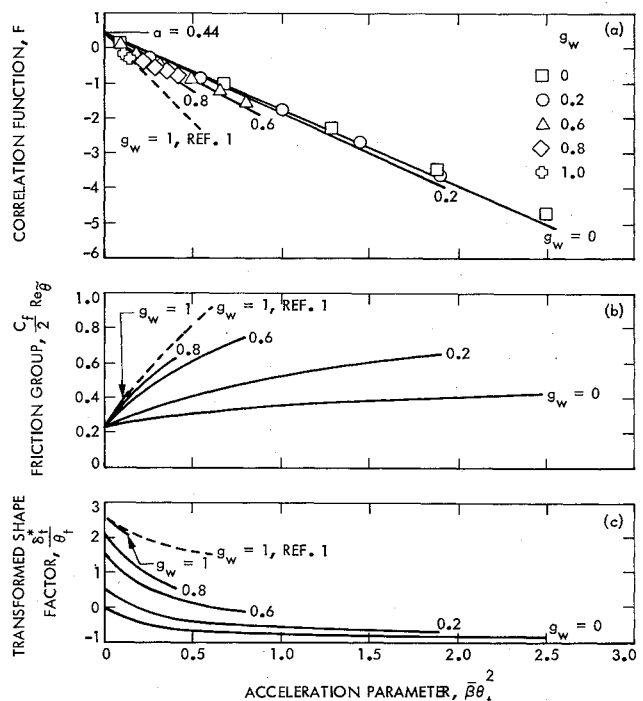


Fig. 1 Variation of the correlation function  $F$ , friction group  $c_f/2 Re_{\bar{\theta}}$ , and transformed shape factor  $\delta_t^*/\theta_t$  with acceleration parameter  $\beta\theta_t^2$  and surface-to-total gas enthalpy parameter  $g_w$ .

permeable surface of negligible curvature for which the integral momentum equation is

$$\frac{d\bar{\theta}}{dx} + \frac{\bar{\theta}}{r_w^j \rho_e u_e^2} \frac{d}{dx} (r_w^j \rho_e u_e^2) + \frac{\bar{\delta}^*}{u_e} \frac{du_e}{dx} = \frac{c_f}{2} \quad (1)$$

In this relation  $j=1$  for an axisymmetric flow and  $j=0$  for flow over a plane surface. The present investigation pertains to larger values of acceleration ( $\bar{\beta}$  to 20 rather than 2) than previously considered<sup>2,3</sup> to account for rapidly accelerating flows such as in supersonic nozzles.

### Approximate Method

The approximate method involves the use of similar solutions in conjunction with the integral momentum equation for isentropic, freestream flow of a perfect gas by assuming that  $\mu \propto T$ , Prandtl number of unity, and  $c_p = \text{const}$ . The similar, boundary-layer velocity and total enthalpy profiles depend upon acceleration and cooling parameters when the combined Levy-Mangler transformation is applied to the differential form of the boundary-layer equations.<sup>4</sup> Equation (1) then can be written in a more convenient form as follows<sup>†</sup>

$$u_e \frac{d}{dx} \left[ \frac{\bar{\theta}^2}{\nu_e} \right] = F(\bar{\beta} \theta_t^2, g_w) - 2 \frac{\bar{\theta}^2}{\nu_e} \frac{u_e}{r_w^j} \frac{dr_w^j}{dx} + \left[ \frac{4\gamma-2}{\gamma-1} \right] \frac{\bar{\theta}^2}{\nu_e} \frac{du_e}{dx} \left[ \frac{T_{To}}{T_e} - 1 \right] \quad (2)$$

where

$$\bar{\beta} \theta_t^2 = \frac{T_{To}}{T_e} \frac{\bar{\theta}^2}{\nu_e} \frac{du_e}{dx}; \quad F(\bar{\beta} \theta_t^2, g_w) = 2 \left[ f_w'' \theta_t - \left( 2 + \frac{\delta_t^*}{\theta_t} \right) \bar{\beta} \theta_t^2 \right] \quad (3)$$

$$\frac{c_f}{2} Re_{\bar{\theta}} = f_w'' \theta_t; \quad \frac{\bar{\delta}^*}{\bar{\theta}} = \frac{T_{To}}{T_e} \left[ 1 + \frac{\delta_t^*}{\theta_t} \right] - 1; \quad \frac{\bar{\delta}}{\bar{\theta}} = \frac{\bar{\delta}^*}{\bar{\theta}} + \frac{\delta_t}{\theta_t} \quad (4)$$

In this formulation  $\bar{\beta} \theta_t^2$  is the acceleration parameter, and the correlation function  $F$  depends only upon  $\bar{\beta} \theta_t^2$  and  $g_w$  (the surface to total gas enthalpy or cooling parameter) from the similar solutions. The other quantities with a subscript  $t$  refer to the following expressions in the transformed coordinate  $\eta$  used in obtaining the similar solutions

$$\theta_t = \int_0^\infty f' (1-f') d\eta; \quad \delta_t^* = \int_0^\infty [G(1-g_w) + g_w - f'] d\eta; \quad \delta_t = \int_0^{\eta^* = 0.99} f' d\eta \quad (5)$$

The similar solutions of Ref. 5 are used in particular because they extend to large values of  $\bar{\beta} \theta_t^2$ . Quantities of interest are given in Table 1 and values of  $F$ , the friction group  $(c_f/2) Re_{\bar{\theta}}$ , and transformed shape factor  $\bar{\delta}_t^*/\theta_t$ , are shown in Fig. 1.

It appears that the linear relation

$$F = a - b[\bar{\beta} \theta_t^2] \quad \text{where } a = 0.44 \quad \text{and } b = b(g_w) \quad (6)$$

<sup>†</sup>In Ref. 3 the density-viscosity product  $\rho_e \mu_e$  in the freestream was taken to be invariable along the flow, but this precludes letting the freestream pressure vary as it would in general. Consequently, the form of the momentum equation in Ref. 3 is different than Eq. (2).

though not exact, is a fair representation of the values shown in Fig. 1. The dependence of  $b$  on  $g_w$  is

$g_w$	0	0.2	0.6	0.8	1.0
$b$	2.2	2.3	2.7	3.4	5.1

Substitution of Eq. (6) into Eq. (2) then permits a simple integration for the variation of the momentum thickness along the surface

$$\frac{\bar{\theta}^2}{\nu_e} = \left[ \frac{2}{\gamma-1} \right]^{s/2} \frac{\left[ 1 + \frac{\gamma-1}{2} M_e^2 \right]^{s/2}}{r_w^{2j} M_e^b} \left\{ \frac{a}{a_{To}} \left[ \frac{\gamma-1}{2} \right]^{s/2} \int_0^x \frac{r_w^{2j} M_e^{b-1}}{\left[ 1 + \frac{\gamma-1}{2} M_e^2 \right]^{(s/2)(s-1)}} dx + c \right\} \quad (7)$$

where  $c$  is a constant of integration to be evaluated at  $x=0$ , and  $s = (4\gamma-2)/(\gamma-1)$ . With the momentum thickness known, the friction coefficient is obtained from Fig. 1b and the displacement thickness from Eq. (4) via Fig. 1c. It is of note that in the low speed limit  $M_e \rightarrow 0$ , Eq. (7) reduces to Eqs. (4) and (6) in Ref. 1 for  $j=0$  and 1, respectively; but when there is heat transfer,  $b$  is no longer equal to 5.15. The dependence of  $b$  on  $g_w$  reflects the influence of heat transfer on the boundary-layer quantities.

### Applications

Confidence in the predictions was established by the relatively good agreement with the centerline temperature measurements by Rothe<sup>6</sup> in a nozzle with a divergent half angle of  $20^\circ$ , an expansion area ratio of  $\epsilon_e = 66$ , a throat diam of  $D_{th} = 2.5$  mm, and at a throat Reynolds number of  $Re_{Dth} = 770$  ( $B = 1230$  in Rothe's nomenclature). These measurements shown in Fig. 2 were obtained with nitrogen at a

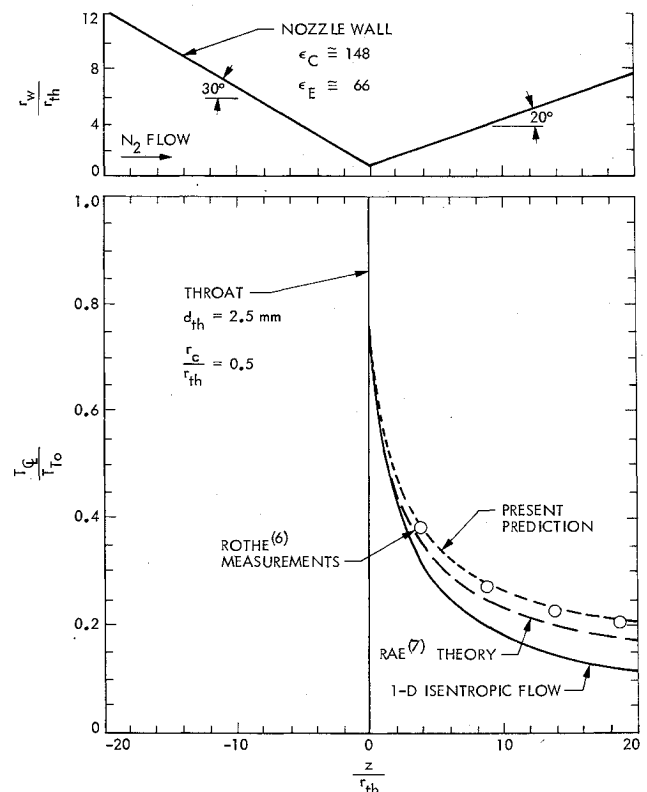


Fig. 2 Comparison between centerline temperature measurements and predictions.

Table 1 Quantities from similar solutions with wall cooling

$g_w$	$\beta$	$\theta_t$	$\beta\theta_t^2$	$\delta_t^*/\theta_t$	$\delta_t/\theta_t$	$f_w''$	$f_w''\theta_t$	$F$
0	0	0.471	0	0	4.81	0.4696	0.221	0.442
	0.5	0.423	0.0896	-0.257	5.09	0.5812	0.246	0.180
	2	0.383	0.294	-0.539	5.47	0.7387	0.283	-0.292
	5	0.365	0.666	-0.711	5.75	0.8907	0.325	-1.066
	10	0.357	1.275	-0.810	5.91	1.0308	0.368	-2.297
	15	0.353	1.874	-0.856	5.97	1.1231	0.397	-3.494
	20	0.353	2.489	-0.880	5.98	1.1935	0.421	-4.732
0.2	0	0.471	0	0.517	4.80	0.4696	0.221	0.442
	0.5	0.409	0.0837	0.199	5.19	0.6550	0.268	0.168
	2	0.355	0.253	-0.166	5.75	0.9483	0.337	-0.253
	5	0.328	0.537	-0.419	6.22	1.2816	0.420	-0.858
	10	0.315	0.991	-0.579	6.51	1.6422	0.517	-1.782
	15	0.310	1.444	-0.656	6.64	1.9114	0.593	-2.694
	20	0.308	1.894	-0.703	6.72	2.1348	0.657	-3.600
0.6	0	0.471	0	1.551	4.80	0.4696	0.221	0.442
	0.5	0.380	0.0721	1.184	5.39	0.7952	0.302	0.145
	2	0.295	0.174	0.763	6.31	1.3334	0.393	-0.174
	5	0.246	0.302	0.414	7.38	1.9824	0.487	-0.483
	10	0.219	0.478	0.142	8.37	2.7162	0.594	-0.860
	15	0.207	0.641	-0.0092	8.91	3.2789	0.678	-1.198
	20	0.200	0.797	-0.110	9.26	3.7528	0.749	-1.514
0.8	0	0.471	0	2.067	4.80	0.4696	0.221	0.442
	0.5	0.365	0.0667	1.721	5.48	0.8623	0.315	0.133
	2	0.263	0.138	1.374	6.45	1.5134	0.398	-0.137
	5	0.202	0.204	1.081	7.69	2.3056	0.466	-0.327
	10	0.167	0.279	0.816	9.19	3.2066	0.536	-0.502
	15	0.152	0.345	0.649	10.23	3.8996	0.591	-0.643
	20	0.142	0.402	0.533	11.00	4.4843	0.636	-0.766
1.0	0	0.471	0	2.590	4.80	0.4696	0.221	0.442
	0.5	0.350	0.0614	2.297	5.56	0.9277	0.325	0.123
	2	0.231	0.106	2.156	6.29	1.6872	0.389	-0.106
	5	0.158	0.125	2.104	6.62	2.6158	0.414	-0.200
	10	0.115	0.132	2.095	6.74	3.6752	0.423	-0.239
	15	0.0951	0.136	2.083	6.80	4.4915	0.427	-0.253
	20	0.0828	0.137	2.075	6.78	5.1807	0.429	-0.260

stagnation temperature of 300°K, for a nearly adiabatic wall, and at a stagnation pressure of 0.020 bar. The present prediction method is in better agreement with the data than Rae's prediction,<sup>7</sup> which is for a wholly viscous flow through a slender nozzle. In the calculations for this relatively low Reynolds number flow, the displacement of the flow external to the boundary layer by the shear layer growth along the wall in the divergent section was taken into account in an iterative way, i.e., the appropriate external flow compatible with the boundary-layer flow is calculated. The external flow was taken to be one-dimensional in the divergent portion of the nozzle. Since the detailed nature of the upstream flow exerts little influence on the flow in the throat region, a displacement thickness correction was not made in the convergent portion of the nozzle, and the Mach number at the edge of the boundary layer was evaluated for one-dimensional flow. The boundary layer was presumed to be of zero thickness at the nozzle inlet. The displacement correction in the throat region determines the appropriate mass flow rate and the effective throat radius on which the calculations in the divergent region are dependent. There are limitations however on the present prediction method at even lower Reynolds numbers where the flow becomes wholly viscous in parts of the nozzle and resort must be made to Rae's prediction.

There is a good agreement between the predicted and measured mass flow rate<sup>6,8</sup> for nozzles with adiabatic walls as indicated in Fig. 3, where flow coefficients are shown. These predicted flow coefficients were obtained via the calculated displacement thickness and inviscid flow coefficient.<sup>9</sup>

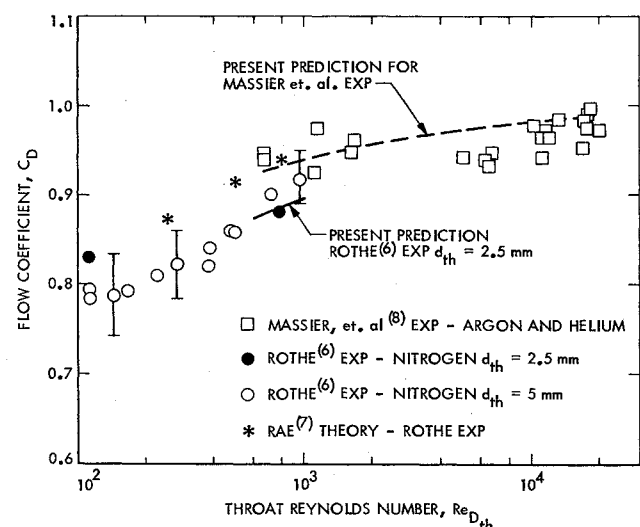


Fig. 3 Measured flow coefficients compared with predictions.

For supersonic nozzle flows with wall cooling,<sup>10</sup> good agreement was found between predicted displacement thicknesses using the procedure of Ref. 2 and values obtained from boundary-layer measurements ( $M_e = 2$  and 10) for the case where selected values of  $b$  were similar in magnitude to those given herein.

$$\left(\frac{dP}{dT}\right)_{\chi_i} = \frac{\Delta S}{\Delta V} \quad (8)$$